AIP | Applied Physics Letters

Structural-induced antiferromagnetism in Mn-based full Heusler alloys: The case of Ni2MnAl

I. Galanakis and E. Şaşıoğlu

Citation: Appl. Phys. Lett. **98**, 102514 (2011); doi: 10.1063/1.3565246
View online: http://dx.doi.org/10.1063/1.3565246
View Table of Contents: http://apl.aip.org/resource/1/APPLAB/v98/i10
Published by the American Institute of Physics.

Structural-induced antiferromagnetism in Mn-based full Heusler alloys: The case of Ni_2MnAl

I. Galanakis[1,a)] and E. Şaşıoğlu[2,b)]
[1]*Department of Materials Science, School of Natural Sciences, University of Patras, GR-26504 Patra, Greece*
[2]*Peter Grünberg Institut and Institute for Advanced Simulation, Forschungszentrum Jülich and JARA, 52425 Jülich, Germany and Department of Physics, Fatih University, Büyükçekmece, 34500 İstanbul, Turkey*

(Received 11 February 2011; accepted 20 February 2011; published online 11 March 2011)

We employ *ab initio* electronic structure calculations and a model Heisenberg Hamiltonian, and show that the Heusler alloy Ni_2MnAl exhibits a ferrromagnetic–antiferromagnetic phase transition upon Mn–Al disorder. The transition is triggered by the smaller Mn–Mn nearest-neighbors distance in accordance to the Bethe–Slater curve. Our results explain available experimental data and show that the prevention of disorder is essential to achieve maximum performance in Heusler-based devices. © *2011 American Institute of Physics*. [doi:10.1063/1.3565246]

Full-Heusler compounds containing Ni and Mn atoms have attracted a lot of attention due to the possibility of observing the shape-memory effect.[1] The magnetic and structural properties in the ferromagnetic (FM) shape-memory alloys (FSMAs) are strongly coupled and the system undergoes a martensitic phase transition presenting unusual magnetomechanical and magnetothermal behavior. The prototype FSMA system is Ni_2MnGa, which shows a large strain effect of 10% in a magnetic field of less than 1 T (Refs. 2 and 3) but it is not suitable for magnetomechanical devices due to the very low temperature, where the martensitic transition occurs, and its brittleness. Several theoretical works have been devoted to the study of its properties.[4,5] Except Ni_2MnGa also other Heusler alloys like $Fe_2CoGa_{1-x}Zn_x$,[6] $(Ni,Co)_2(Mn,Fe)(Ga,Si)$,[7] Co_2NiGa,[8] $Ni_{50}Mn_{50-x}Sn(In)_x$,[9] and $Ni_{50}Mn_{25+x}(In,Sn,Sb)_{25-x}$ (Ref. 10) have been proposed to exhibit the shape-memory effect.

As a promising alternative to Ni_2MnGa, the isovalent Ni_2MnAl Heusler compound has been proposed.[11] In its stoichiometric concentration Ni_2MnAl is structurally stable down to low temperatures and at its slightly off-stoichiometric composition it presents a high-temperature martensitic phase transition while its mechanical properties are superior to Ni_2MnGa.[12] Ni_2MnAl in the B2 phase, where the Ni atoms form a cubic lattice while Mn and Al atoms occupy the other sites randomly (for a discussion of the structure see later in the text), is a conical antiferromagnet[13] and in the perfectly ordered $L2_1$ structure evidence for a FM ordering exist from calorimetric measurements.[14] In 2002 Acet and collaborators studied single crystals of Ni_2MnAl using different annealing temperatures.[15] They found that for the high-temperature annealed sample an antiferromagnetic (AFM) B2 structure was stabilized but for the lower-temperature sample even after 30 days of annealing they were not able to produce a perfect $L2_1$ sample due to the slow kinetics for this compound and the latter was containing inclusions of the B2 phase. The Néel temperature for the AFM B2 phase was found to be 313 K and the Curie temperature for the FM $L2_1$ phase 375 K. Similar results were also produced by Dong *et al.* in the case of thin films of Ni_2MnAl grown on GaAs(001) using molecular beam epitaxy and no sole $L2_1$ phase could be produced.[16] The competition between the FM and AFM ordering has been also observed on films by Paduani *et al.*[17] A mixed $Ni_2Mn(Ga_xAl_{1-x})$ alloy has been also proposed as an intermediate way to combine the mechanical properties of Ni_2MnAl and the easily achieved ordering of the $L2_1$ structure in Ni_2MnGa which is essential for the martensitic transition to occur.[18] The mixed $B2/L2_1$ of Ni_2MnAl has been used to produce negative magnetoresistance ratio in granular films.[19]

First-principles calculations by Enkovaara *et al.* on Ni_2MnAl have confirmed the FM character of the $L2_1$ structure,[20] while Büsgen and collaborators have shown that the $Ni_{50}Mn_xAl_{50-x}$ is FM from 14 to 31 at. % of Mn.[21] But the question of the exact mechanism leading to the AFM order in the B2 structure remains still unanswered although the hypothesis that this is a structural effect is widely assumed in literature. The aim of our letter is to show by first-principles calculations that when the B2 structure occurs the smaller neighboring Mn–Mn distance with respect to the $L2_1$ phase, leads to the stabilization of an AFM interaction as predicted by the Bethe–Slater curve.[22] Thus the appearance of AFM order is not restricted only to Ni_2MnAl but occurs in any B2 Mn-based Heusler alloy destroying the FM order of perfect $L2_1$ films and degrading the performance of potential devices. We calculate the exchange interactions between the Mn atoms following the same methodology as in Ref. 23. We use the augmented spherical waves *ab initio* method[24] within the atomic-sphere approximation[25] to calculate the electronic structure. The exchange-correlation potential is chosen in the generalized gradient approximation[26] and a dense Brillouin zone sampling of $30\times30\times30$ is used. To calculate the interatomic exchange interactions we use the frozen-magnon technique[27] and map the results of the calculation of the total energy of the helical magnetic configurations onto a classical Heisenberg Hamiltonian $H_{\text{eff}}=-\Sigma_{i\neq j}J_{ij}\mathbf{s}_i\mathbf{s}_j$, where J_{ij} is the exchange interaction between two Mn sites and $\mathbf{s}_i$ is the unit vector pointing in the direction of the magnetic moment at site i.

a)Electronic mail: galanakis@upatras.gr.
b)Electronic mail: e.sasioglu@fz-juelich.de.

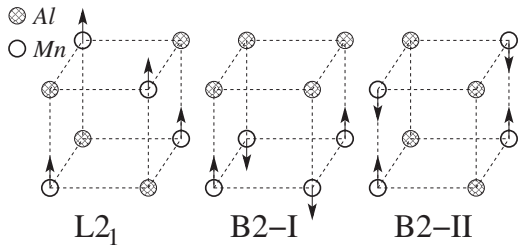

FIG. 1. Al and Mn atoms in Ni_2MnAl form a cubic lattice. We show the perfect $L2_1$ structure and the two types of the B2 structure which we considered. Arrows indicate the calculated orientation of the Mn spin magnetic moments. For the experimental lattice constant a of 5.812 Å,[15] the Mn–Mn nearest-neighbors distance in the B2 structure is $a/2=2.906$ Å while in the $L2_1$ structure it is $a\sqrt{2}/2=4.110$ Å.

The $L2_1$ structure adopted by full-Heusler compounds like Ni_2MnAl consists of four interpenetrating fcc sublattices (see Fig. 1 in Ref. 23) of which two are occupied by Ni atoms and the other two by Mn and Al ones. If we neglect the Ni atoms, Mn and Al form a cubic lattice presented in Fig. 1 and each Mn and Al atom has eight Ni atoms at the centers of the presented cubes (not shown here) as nearest neighbors. In the disordered B2 structure Mn and Al occupy this cubic lattice randomly. Since we have to perform ordered calculations to calculate the exchange constants, we have considered two limiting cases, the B2-I where all Mn atoms are in the same (001) plane and B2-II where all Mn atoms are in the same (110) plane. The main difference between these structures is the Mn–Mn distance. In the $L2_1$ structure the nearest Mn atoms are separated by a $a\sqrt{2}/2$ distance where a is the lattice constant of Ni_2MnAl while in the two B2 structures under consideration the closest Mn–Mn distance is $a/2$. The difference between B2-I and B2-II is the local environment of each atom as can be seen in Fig. 1. For our calculations we have used the experimental lattice constant of 5.812 Å extracted by Acet *et al.*[15]

We performed self-consistent electronic structure calculations for the three structures in Fig. 1 and in Table I we have gathered the calculated atomic spin moments. Note that for each of the three structures, all Mn atoms are equivalent between them. The Mn atoms carry the spin magnetic moment which is about $3.6\mu_B$ in all cases and thus almost insensitive to the structure. Al atoms present a very small induced spin moment antiparallel to the Mn one (for an explanation see Ref. 28). In the $L2_1$ structure we converged to a FM solution with a total spin magnetic moment of $4.1\mu_B$ close to the value calculated in Ref. 28 (see this reference for an extensive discussion on the magnetism of the perfectly ordered FM Ni_2MnAl alloy) and Ni carries a small positive spin moment, while in the two B2 cases we converged to an AFM solution and thus the total spin magnetic moment in the unit cell is zero. Ni atoms in the B2 structures also carry a zero net spin magnetic moment since each Ni is surrounded due to symmetry by an equal number of Mn atoms with positive and negative spin magnetic moments. In Fig. 1 we present with arrows the orientation of the spin magnetic moment of each Mn atom. In the B2 cases nearest-neighboring Mn atoms have opposite spin magnetic moments of the same magnitude. To conclude our discussion on the electronic properties we present also in Fig. 2 the density of states (DOS) for the Ni and Mn atoms in the three studied magnetic structures (for the B2 ones we consider a Mn atom with positive spin moment). The Ni atoms in the AFM cases show a perfectly symmetric DOS for the two spin directions while for the FM case it forms common d-bands with the Mn atom. As discussed in Ref. 28 it is not a half-metallic system in the FM case since it has 30 valence electrons but contrary to the isovalent Co_2FeSi the exchange-splitting of Ni majority- and minority-spin bands is not strong enough to keep the Fermi level within the minority gap and minority-spin conduction states above the minority gap are populated (the gap is located at about -1 eV).

TABLE I. Calculated spin magnetic moments in μ_B for the Ni_2MnAl alloy and the calculated Curie ($L2_1$) and Néel (B2) temperatures within the random-phase-approximation. Experimental temperatures (last column) are from Ref. 15.

Structure	m^{Ni}	m^{Mn}	m^{Al}	m^{Total}	$T_{C,N}^{RPA}$ (K)	$T_{C,N}^{EXP}$ (K)
$L2_1$	0.32	3.54	−0.08	4.10	368	375
B2-I	0.00	3.60	−0.01	0.00	245	313
B2-II	0.00	3.61	−0.05	0.00	350	313

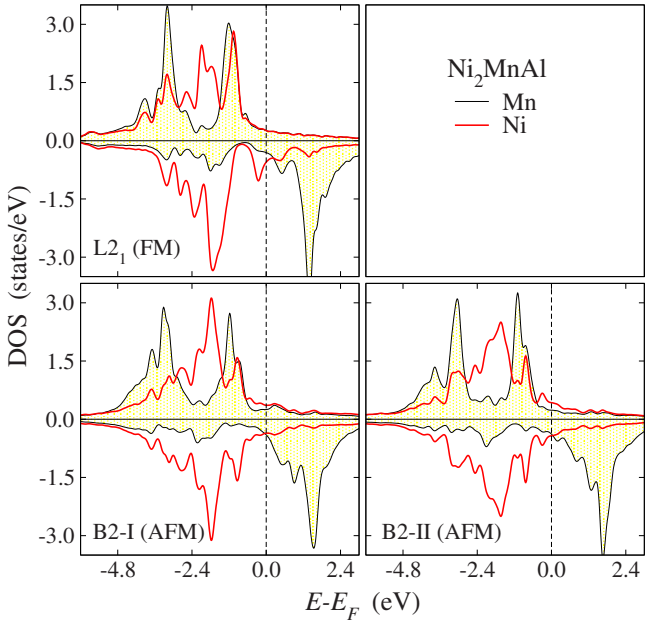

FIG. 2. (Color online) Calculated atom-resolved DOS for the three lattice structures under study. Positive values of the DOS correspond to the majority- and negative to the minority-spin electrons.

In Fig. 3 we present the Mn–Mn exchange constants as a function of the Mn–Mn distance. In the $L2_1$ structure the Mn-Mn nearest neighbors present a FM coupling which persists up to the fifth Mn–Mn neighbors and thus the tendency to ferromagnetism is very strong. On the contrary, in both B2 cases the Mn–Mn nearest neighbors present a negative exchange constant, J_1, which almost vanishes when we move to next-nearest Mn–Mn neighbors but the absolute value for J_1 in the AFM cases is eight times the value of J_1 for the FM case. Thus the AFM order is exclusively due to the nearest-neighboring Mn–Mn interactions. This picture is consistent with the Bethe–Slater curve for transition metals which represents the behavior of the exchange energy as a function of the ratio of the nearest-neighbors distance over the radius of the d-orbitals.[22] When the ratio is close to γ-Fe we have a spin-glass state. When it decreases, the exchange energy becomes negative leading to an AFM state while when the ratio

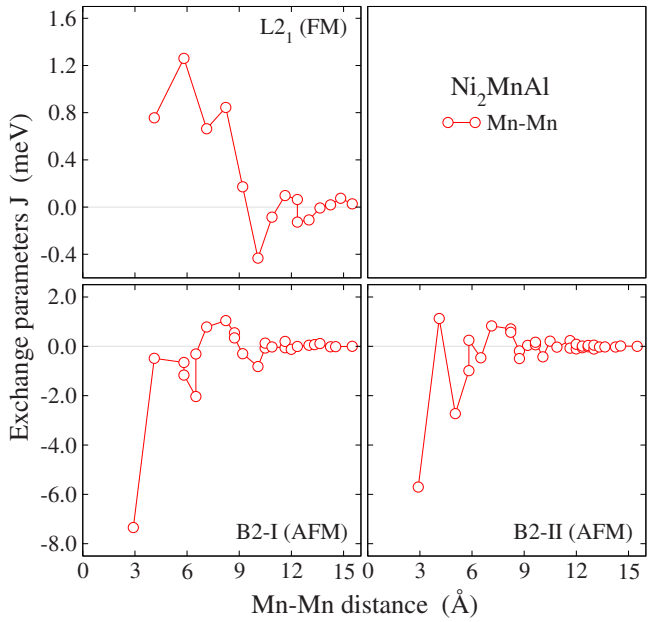

FIG. 3. (Color online) Calculated Mn–Mn exchange constants as a function of the distance.

increases the exchange energy becomes positive leading to a FM case. Thus when we pass from the $L2_1$ to the B2 structure the Mn–Mn nearest neighbors decreases by a factor of $1/\sqrt{2}$ and AFM is stabilized. Finally, we have used the exchange constants to calculate the Curie temperature, T_C, in the FM-$L2_1$ and the Néel temperature, T_N, in the AFM-B2 cases in the random phase approximation[23] and we present our results in Table I. Our calculated T_C is 368 K close to the experimental value of 375 K (Ref. 15) while for the B2-I and B2-II structure the T_N is 245 K and 350 K, respectively, close to the value of 313 K for the fully disordered B2 single crystal.[15]

Employing *ab initio* electronic structure calculations in conjunction with a model Hamiltonian, we have demonstrated a structural-driven magnetic phase transition in the Ni_2MnAl Heusler alloy. When Mn atoms exchange sites with Al ones, destroying the perfect $L2_1$ order and establishing the B2 disordered lattice, the smaller Mn–Mn distance leads to an AFM interaction and to a magnetic phase transition. Our results explain the experimental results in the case of Ni_2MnAl single crystals and films in Refs. 15 and 16, where the mixed $L2_1$/B2 samples were found to contain both FM and AFM domains. Results are of importance for the whole community trying to incorporate Mn-based Heusler films and multilayers in functional spintronic devices since a small degree of disorder during growth can degrade the FM properties of the film/multilayer.

Fruitful discussions with L. M. Sandratskii are gratefully acknowledged.

[1]L. Mañosa, X. Moya, A. Planes, T. Krenke, M. Acet, and E. F. Wassermann, Mater. Sci. Eng., A **481–482**, 49 (2008).
[2]S. J. Murray, M. Marioni, S. M. Allen, and R. C. O'Handley, Appl. Phys. Lett. **77**, 886 (2000).
[3]K. Ullakko, J. K. Huang, C. Kanter, R. C. O'Handley, and V. Kokorin, Appl. Phys. Lett. **69**, 1966 (1996).
[4]A. T. Zayak, P. Entel, J. Enkovaara, A. Ayuela, and R. M. Nieminen, Phys. Rev. B **68**, 132402 (2003).
[5]V. D. Buchelnikov, V. V. Sokolovskiy, H. C. Herper, H. Ebert, M. E. Gruner, S. V. Taskaev, V. V. Khovaylo, A. Hucht, A. Dannenberg, M. Ogura, H. Akai, M. Acet, and P. Entel, Phys. Rev. B **81**, 094411 (2010).
[6]A. Dannenberg, M. Siewert, M. E. Gruner, M. Wuttig, and P. Entel, Phys. Rev. B **82**, 214421 (2010).
[7]S. E. Kulkova, S. V. Eremeev, S. S. Kulkov, and V. A. Skripnyak, Mater. Sci. Eng., A **481–482**, 209 (2008).
[8]M. Siewert, M. E. Gruner, A. Dannenberg, A. Hucht, S. M. Shapiro, G. Xu, D. L. Schlagel, T. A. Lograsso, and P. Entel, Phys. Rev. B **82**, 064420 (2010).
[9]X. Moya, L. Mañosa, A. Planes, T. Krenke, M. Acet, and E. F. Wassermann, Mater. Sci. Eng., A **438–440**, 911 (2006).
[10]V. D. Buchelnikov, P. Entel, S. V. Taskaev, V. V. Sokolovskiy, A. Hucht, M. Ogura, H. Akai, M. E. Gruner, and S. K. Nayak, Phys. Rev. B **78**, 184427 (2008).
[11]T. Mehaddene, J. Neuhaus, W. Petry, K. Hradil, P. Bourges, and A. Hiess, Phys. Rev. B **78**, 104110 (2008).
[12]X. Moya, L. Mañosa, A. Planes, T. Krenke, M. Acet, M. Morin, J. L. Zarestky, and T. A. Lograsso, Phys. Rev. B **74**, 024109 (2006).
[13]R. R. A. Ziebeck and P. J. Webster, J. Phys F: Met. Phys. **5**, 1756 (1975).
[14]F. Gejima, Y. Sutou, R. Kainuma, and K. Ishida, Metall. Mater. Trans. A **30**, 2721 (1999).
[15]M. Acet, E. Duman, E. F. Wassermann, L. Mañosa, and A. Planes, J. Appl. Phys. **92**, 3867 (2002).
[16]X. Y. Dong, J. W. Dong, J. Q. Xie, T. C. Shih, S. McKernan, C. Leighton, and C. J. Palmstrom, J. Cryst. Growth **254**, 384 (2003).
[17]C. Paduani, A. Migliavacca, M. L. Sebben, J. D. Ardisson, M. I. Yoshida, S. Soriano, and M. Kalisz, Solid State Commun. **141**, 145 (2007).
[18]H. Ishikawa, R. Y. Umetsu, K. Kobayashi, A. Fujita, R. Kainuma, and K. Ishida, Acta Mater. **56**, 4789 (2008).
[19]A. Vovk, M. Yu, L. Malkinski, C. O'Connor, Z. Wang, E. Durant, J. Tang, and V. Golub, J. Appl. Phys. **99**, 08R503 (2006).
[20]J. Enkovaara, A. Ayuela, J. Jalkanen, L. Nordström, and R. M. Nieminen, Phys. Rev. B **67**, 054417 (2003).
[21]T. Büsgen, J. Feydt, R. Hassdorf, S. Thienhaus, M. Moske, M. Boese, A. Zayak, and P. Entel, Phys. Rev. B **70**, 014111 (2004).
[22]D. Jiles, *Introduction to Magnetism and Magnetic Materials* (Chapman & Hall, London, 1998).
[23]E. Şaşıoğlu, L. M. Sandratskii, P. Bruno, and I. Galanakis, Phys. Rev. B **72**, 184415 (2005).
[24]A. R. Williams, J. Kübler, and C. D. Gelatt, Phys. Rev. B **19**, 6094 (1979).
[25]O. K. Andersen, Phys. Rev. B **12**, 3060 (1975).
[26]J. P. Perdew and Y. Wang, Phys. Rev. B **45**, 13244 (1992).
[27]L. M. Sandratskii and P. Bruno, Phys. Rev. B **66**, 134435 (2002); L. M. Sandratskii, Adv. Phys. **47**, 91 (1998).
[28]I. Galanakis, P. H. Dederichs, and N. Papanikolaou, Phys. Rev. B **66**, 174429 (2002).